Measuring axial and radial diffusivities in the brain.

C. A. Wheeler-Kingshott[1], D. C. Alexander[2], T. Schneider[1], and M. Cercignani[3]

[1]Department of Neuroinflammation, UCL Institute of Neurology, London, United Kingdom, [2]Dept. Computer Science, University College London, Centre for Medical Image Computing, London, United Kingdom, [3]Neuroimaging Laboratory, Fondazione Santa Lucia, Rome, Italy

Introduction: Axial and radial diffusivities, i.e. the water diffusion coefficient measured along and across a white matter tract, have been associated with the principal eigenvector of the diffusion tensor and the average of its orthogonal components[1]. This is an acceptable approximation if the voxel contains a healthy fiber bundle that determines the diffusion properties of the voxel, but can lead to misinterpretation of the results if signal-to-noise is low, or if crossing fibers are present or if pathology causes a decrease in anisotropy, because in each of these situations the directionality of the principal diffusivity becomes more arbitrary[2], i.e. it may be aligned with a direction other than that of the underlying "healthy" structure. In such voxels, comparing the principal eigenvector of the DT of healthy controls and of patients with lesions, such as in multiple sclerosis (MS), can be misleading because it corresponds to effectively comparing the diffusion coefficient along two different directions. This work shows a way to determine the axial and radial diffusivities consistently between subjects by using a healthy-subjects "super-dataset" created from a control population representing the subjects under study to define the orientation for diffusivity comparisons.

Methods: Acquisition - DTI datasets were acquired on 11 healthy controls (5 males and 6 females, mean age 41±8 years) with a cardiac gated DT-EPI sequence (22cm FOV, 96x96 matrix, 2.3x2.3x2.3mm^3 voxel size reconstructed to 1.87x1.87x2.3mm^3, 60 contiguous slices aligned with the AC-PC line, 96ms TE and 20RR TR, 68 diffusion-weighted scans with 7 b=0 and 61 b=1200 smm^{-2} along uniformly distributed directions). Data processing - The processing pipeline followed these steps: i) Data was corrected for eddy currents induced distortions using the FSL package (http://www.fmrib.ox.ac.uk/fsl/fdt/index.html); (ii) The DT was determined in native space for each subject using Camino (http://www.camino.org.uk); (iii) Fractional Anisotropy (FA) maps were non-linearly registered to the FMRIB FA template (FA_{FMRIB}) using FNIRT (part of the FSL package) with a resolution of 1x1x1mm^3; (iv) The components of the non-diagonalised DT (ii) were then transformed into the standard space by applying the transformations of step (iii) followed by the application of the preservation of principal direction (PPD) algorithm[3] in Camino, resulting in a DT dataset in FA_{FMRIB} space, DT_{FMRIB}; (v) The DT_{FMRIB} datasets for the 11 subjects were subsequently averaged to lead to a DT_{AV} dataset representing the population under investigation; (vi) The DT_{FMRIB} and the DT_{AV} dataset were each diagonalised to produce the eigenvalues ($\lambda_{1,i}$, $\lambda_{2,i}$, $\lambda_{3,i}$) and eienvectors ($\mathbf{v}_{1,i}$, $\mathbf{v}_{2,i}$, $\mathbf{v}_{3,i}$) of the DT in FA_{FMRIB} space for each subject and for the average dataset, with i = (1-11, AV). Axial diffusivity – The DT_{AV} dataset was considered the "gold-standard" given its high signal-to-noise ratio (SNR) and it was assumed that its principal eigenvector $\mathbf{v}_{1,AV}$ represented the principal direction of diffusivity determined by the underlying fiber bundles. To determine the axial diffusivity $d_{axial,i}$ for each individual subject, i, we calculated the component of each subject's $DT_{FMRIB,i}$ along $\mathbf{v}_{1,AV}$ as follows:

$$d_{axial,i} = (\mathbf{v}_{1,AV})^T \cdot D_{FMRIB,i} \cdot (\mathbf{v}_{1,AV}).$$

Radial diffusivity – We calculated the radial diffusivity as the average of the projection of $DT_{FMRIB,i}$ along $\mathbf{v}_{2,AV}$ and $\mathbf{v}_{3,AV}$ as follows:

$$d_{radial,i} = ((\mathbf{v}_{2,AV})^T \cdot D_{FMRIB,i} \cdot (\mathbf{v}_{2,AV}) + (\mathbf{v}_{3,AV})^T \cdot D_{FMRIB,i} \cdot (\mathbf{v}_{3,AV}))/2.$$

Results: Maps of $d_{axial,i}$ and of $d_{radial,i}$ are compared to maps of $\lambda_{1,i}$ and of $(\lambda_{2,i}+\lambda_{3,i})/2$. In the healthy subjects of this study and in the core of white matter tracts, the values of $d_{axial,i}$ are consistent with $\lambda_{1,i}$ as are the values of of $d_{radial,i}$ with $(\lambda_{2,i}+\lambda_{3,i})/2$, but colour maps of the direction of the eigenvector $\mathbf{v}_{1,i}$ modulated with $\lambda_{1,i}$ (figure 1, a-b-c) and of $\mathbf{v}_{1,AV}$ modulated with $d_{axial,i}$ (figure 1, a'-b'-c') show the superior definition of the different white matter bundles when calculating the axial diffusivities based on the eigenvectors obtained from the super-dataset, $DT_{FMRIB,AV}$. The radial diffusivity calculated along the directions of the second and third eigenvector of $DT_{FMRIB,AV}$ shows similar improvement over $(\lambda_{2,i}+\lambda_{3,i})/2$.

Conclusions: We have presented a method for calculating the axial and radial diffusivities based on a high-SNR healthy dataset representing the population under investigation. This development allowed us to compute d_{axial} and d_{radial} consistently across a population. This method overcomes the problems associated with the uncertainlty of the eigenvectors' direction especially in regions of low SNR and in areas affected by pathology when comparing patients and controls axial and radial diffusivities. The problems associated with crossing fibers, instead, still remain unsolved, but if non-diffusion tensor methods of data processing were going to be used on the healthy super-dataset, multi-directional information would become available for characterisation of tract-specific axial and radial diffusivities, overcoming the directional uncertainty of voxels containing crossing fibers.

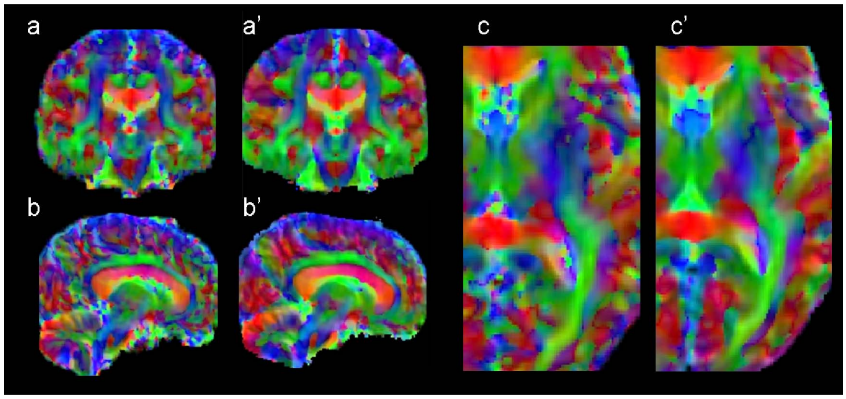

Figure 1: a-b-c) Directionality map of the principal eigenvector of the $DT_{FMRIB,i}$, $\mathbf{v}_{1,i}$ for subject i modulated with the corresponding principal eigenvalues $\lambda_{1,i}$.
a'-b'-c') Directionality map of the principal eigenvector of the $DT_{FMRIB,AV}$, $\mathbf{v}_{1,AV}$, modulated with the axial diffusivity, $d_{axial,i}$.

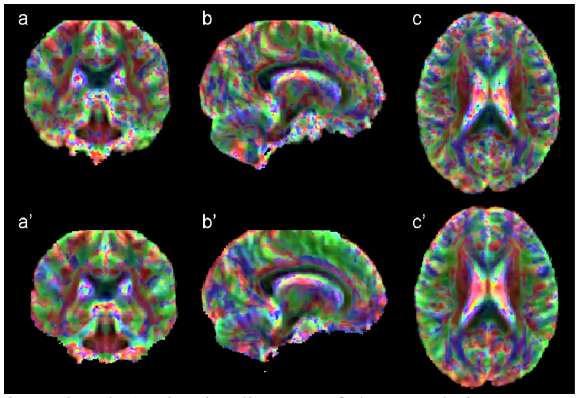

Figure 2: a-b-c) Directionality map of the second eigenvector of $DT_{FMRIB,i}$, $\mathbf{v}_{2,i}$ for subject i modulated with the mean of the second and third eigenvalues, $(\lambda_{2,i}+\lambda_{3,i})/2_i$.
a'-b'-c') Directionality map of the second eigenvector of $DT_{FMRIB,AV}$, $\mathbf{v}_{2,AV}$, modulated with the radial diffusivity, $d_{radial,i}$.

References: 1. Song et al. Neuroimage. 20,1714(2003); 2. Wheeler-Kingshott & Cercignani. Proc. of the XVI meeting of the ISMRM, 3271 (2008); 3. Alexander et al. IEEE Trans. Med. Imaging 20, 1131 (2001).

Acknowledgements: The Multiple Sclerosis Society of Great Britain and Northern Ireland for funding. Declan Chard and Ulrike Bonati for providing the data.